
An Alternative Model for Zika Virus

Justin Sullivan

Abstract

In this paper, an alternative to an existing deterministic model for Zika Virus is proposed. In the original model, individual measures to protect against the virus are taken into account via a constant transfer rate from the susceptible population to the recovered population. The proposed model accounts for these measures via limiting parameters attached to the transmission probability of the virus; one parameter limits the probability of vector transmission through the use of PPE, while the other limits the probability of sexual transmission. The proposed model possesses a disease-free equilibrium that is locally, asymptotically stable when the basic reproductive number is less than one. In order to compare the efficacy of the new model to that of the original, both systems were given identical parameter values and their graphs and point-estimates were compared. For reasonable values of the new limiting parameters, both models produce nearly-identical graphs and point estimates. In addition, for identical parameter values and initial conditions, elasticity analysis determined that the limiting parameter associated with the probability of vector-transmission was far more influential on the new system than the parameter used in the original model.

Introduction

The effects of climate change in the United States, particularly in the state of Florida, are creating ideal conditions for mosquito populations to thrive. As the populations of certain breeds increase, particularly those of the *Aedes aegypti* and *Aedes albopictus*, so does the risk of experiencing a major outbreak of the various diseases that they carry [11]. These mosquitos are two of the primary vectors associated with several emerging tropical diseases, including Dengue, Yellow Fever, Chikungunya, and Zika Virus. It is the association between Zika Virus and conditions such as Guillain Barré Syndrome and Microcephaly that have caused it to be the subject of this paper [5,6].

Zika Virus is an emerging tropical disease that is transmissible through infectious vectors, sexual interaction with an infected host, and vertical transmission; the primary vector for the virus is the female *Aedes aegypti* mosquito [4]. The symptoms associated with the virus tend to be very mild, ranging from low-grade fever and rash to muscle pain and conjunctivitis, though many people who contract Zika show no symptoms at all [7].

First discovered by scientists in Uganda in 1947, the largest outbreak of the disease occurred in Brazil beginning in the year 2015. Throughout the first eleven months of 2016, the outbreak was considered a Public Health Emergency of International Concern by the World Health Organization (WHO) [9]. In November of 2016, the WHO ended its decree of Zika as a Public Health Emergency. Though scientists are not exactly sure what interrupted the transmission of the virus, it is speculated to have been caused by population immunity, given that over 200,000 cases of Zika Virus were reported in Brazil that year [8].

Since the outbreak, many mathematical models have been put forth for Zika Virus. Given its many modes of transmission, these models very rarely take into account all three at the same time. Though models that only account for one mode of transmission do exist, the majority attempt to model the virus with two transmission routes [1,3,10,12]. Additionally, many of existing models use an SEIR vector-host format,

with some adding an asymptomatic class to account for infected individuals who do not exhibit symptoms of the virus. The model under observation for this paper, created by Biswas, Gosh, and Sakar (2019), uses the described format, without consideration for asymptomatic individuals, and accounts for vector transmission, sexual transmission, and vector control [2]. This model will be referred to as the “original model” for the remainder of this paper.

In the original model, personal protective measures against the virus are taken into account; it is the way in which this is done, however, that has prompted this study. In the original model, susceptible hosts are removed at a constant rate α and placed directly into the recovered class, under the assumption that the host population will take steps to protect themselves against the virus as they become more aware of its risks. This constant removal is demonstrated by the red arrow in the model’s flow diagram, shown in [Figure 1](#). By accounting for precautionary measures in this manner, three immediate consequences become evident:

- The host population flows through the model in a way that goes against basic intuition about disease spread.
- Susceptible and recovered host populations become inaccurate.
- The ability to account for specific precautionary measures, against both the vector and sexual transmission routes, is not possible.

The remainder of this paper will seek to discuss the results of modifying this model in a way that aims to make it both more accurate and more intuitive, by removing the jump from the susceptible to recovered class and, instead, introducing parameters that suppress the vector and sexual transmission rates of Zika separately.

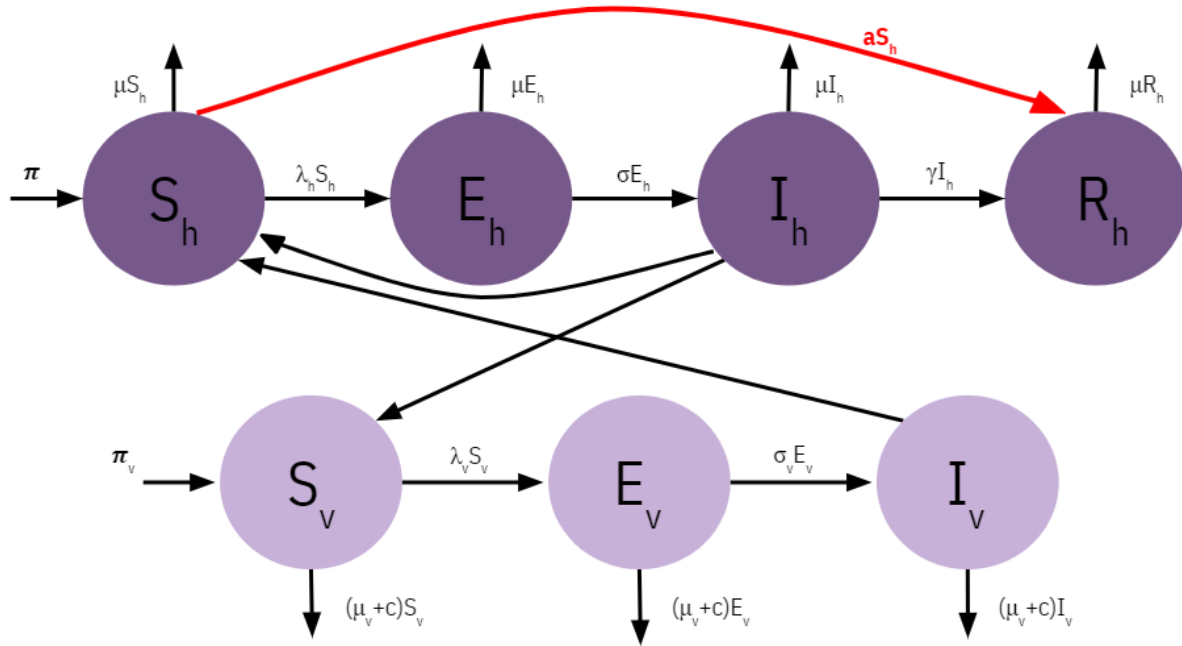


Figure 1. Flow diagram of the proposed model for Zika Virus with vector and sexual transmission routes considered.

Model

As stated in the previous section, the purpose of this project was to discover whether the original model could be modified to increase its accuracy and interpretability, without losing the ability to analyze it. In order to formulate the modified model, the following assumptions were made:

- The birthing rates for both the vector and hosts populations are constant.
- The natural death rates for both the vector and hosts populations are constant.
- Vector population control measures have a constant rate of efficacy.
- Zika Virus does not cause death in either population.

[Figure 2](#) represents the flow diagram for the proposed model. In the figure, progression rates between classes are labelled; furthermore, it should be noted that the flow diagrams for both models are identical except for the presence of the red arrow in that of the original model.

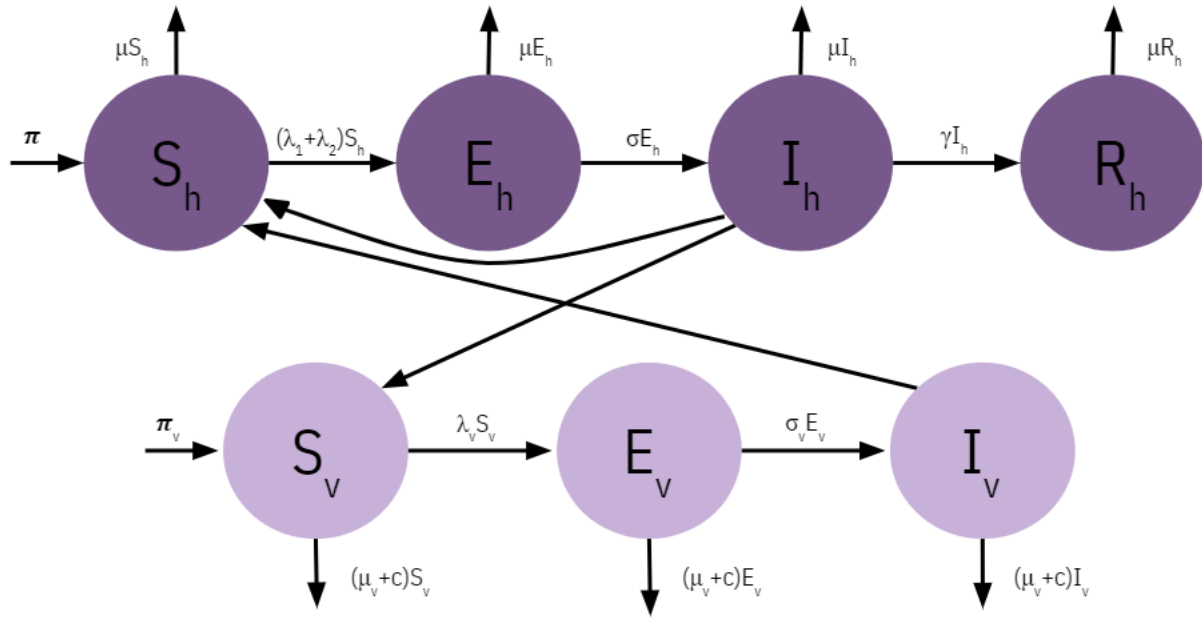


Figure 2. Flow diagram of the proposed model for Zika Virus with vector and sexual transmission routes considered.

In order to allow for this removal of the jump from the susceptible to recovered class, the virus's transmission rate λ was altered slightly. Since two modes of host transmission are considered in each model, let λ be equal to the sum of λ_1 and λ_2 , which represent the host transmission rates due to vector and sexual transmission, respectively. In the proposed model, λ_1 and λ_2 have been modified to include parameters that reduce their values, based on the efficacy of introduced control measures. To λ_1 , the rate of transmission due to vectors, the parameter k_v was introduced and can be calculated based on the effectiveness of precautionary measures that reduce the biting rate of mosquitos, including bug sprays and mosquito nets. To λ_2 , the rate of sexual transmission, the parameter k_s was introduced and can be determined from the efficacy of measures that reduce the sexual transmission rate, such as reducing one's

number of sexual partners or increasing the use of condoms during sexual intercourse. It is worth noting that the definitions of λ_1 and λ_2 are identical in both models except for the introduction of the two new parameters in the proposed model.

In the system, let $\lambda = \lambda_1 + \lambda_2$ represent the overall host transmission rate of the virus, where $\lambda_1 = \frac{k_v b \alpha_1 I_v}{N_h}$ and $\lambda_2 = \frac{k_s r \alpha_2 I_h}{N_h}$. Furthermore, let $\lambda_v = \frac{b \alpha_3 I_h}{N_h}$ be the rate at which susceptible vectors become exposed to the virus via an infected host. Finally, let $N_h = S_h + E_h + I_h + R_h$ represent the entire host population under consideration. The following system of non-linear differential equations in the left column serves to depict the model in its entirety, while the equations in the right column define each of the transmission routes; additionally, a list of all parameters used can be found in [Table 1](#).

$$\left\{ \begin{array}{l} \frac{dS_h}{dt} = \pi - (\lambda_1 + \lambda_2)S_h - \mu S_h \\ \frac{dE_h}{dt} = (\lambda_1 + \lambda_2)S_h - (\sigma + \mu)E_h \\ \frac{dI_h}{dt} = \sigma E_h - (\gamma + \mu)I_h \\ \frac{dR_h}{dt} = \gamma I_h - \mu R_h \\ \frac{dS_v}{dt} = \pi_v - \lambda_v S_v - (\mu_v + b)S_v \\ \frac{dE_v}{dt} = \lambda_v S_v - (\sigma_v + \mu_v + c)E_v \\ \frac{dR_v}{dt} = \sigma_v E_v - (\mu_v + c)I_v \end{array} \right. \quad \left\{ \begin{array}{l} \lambda_1 = \frac{k_v b \alpha_1 I_v}{N_h} \quad (\text{vector} \rightarrow \text{host}) \\ \lambda_2 = \frac{k_s r \alpha_2 I_h}{N_h} \quad (\text{host} \rightarrow \text{host}) \\ \lambda_v = \frac{b \alpha_3 I_h}{N_h} \quad (\text{host} \rightarrow \text{vector}) \end{array} \right.$$

Table 1. Description of parameters used in model	
Parameter	Description
b	Biting rate of mosquitos
c	Rate of vector control
k_s	Limiting parameter for sexual transmission rate $(1 - \varepsilon_s)$
k_v	Limiting parameter for vector transmission rate $(1 - \varepsilon_v)$
r	Sexual contact rates between hosts
α_1	Probability of transmission from infected vector to susceptible host
α_2	Probability of transmission from infected host to susceptible vector
α_3	Probability of sexual transmission from infected host to susceptible host
γ	Recovery rate of infected host
ε_s	Effectiveness of precautionary measures against sexual transmission
ε_v	Effectiveness of precautionary measures against vector transmission
μ, μ_v	Natural death rates for host and vector populations, respectively
π, π_v	Natural birth rates for host and vector populations, respectively
σ, σ_v	Progression rates from E to I class for host and vector populations, respectively

System Analysis

In this section, the system's basic reproductive number, \mathcal{R}_0 , and the local asymptotic stability of its disease-free equilibrium (DFE) are discussed.

To obtain the system's DFE, let $E_h = I_h = E_v = I_v = 0$, so that

$$DFE(S_h^0, E_h^0, I_h^0, R_h^0, S_v^0, E_v^0, I_v^0) = \left(\frac{\pi}{\mu}, 0, 0, \frac{\pi}{\mu^2}, \frac{\pi_v}{\mu_v + c}, 0, 0\right) \quad (1)$$

Due to the size of the system being studied, the next generation method was necessary to determine its basic reproductive number. For this calculation, two Jacobian matrices, F and V , were constructed that

capture new infections in the E_h and E_v classes, as well the flow of existing infections through the E_h , I_h , E_v , I_v classes, respectively, at the DFE.

$$F = \begin{bmatrix} 0 & \lambda_2^0 S_h^0 & 0 & \lambda_1^0 S_h^0 \\ 0 & 0 & 0 & 0 \\ 0 & \lambda_v^0 S_v^0 & 0 & 0 \\ 0 & 0 & 0 & 0 \end{bmatrix} \quad \text{and} \quad V = \begin{bmatrix} k_1 & 0 & 0 & 0 \\ -\sigma & k_2 & 0 & 0 \\ 0 & 0 & k_3 & 0 \\ 0 & 0 & -\sigma_v & k_4 \end{bmatrix} \quad (2)$$

From there, the basic reproductive number is determined to be the spectral radius, ρ , also known as the dominant eigenvalue of the matrix $K = FV^{-1}$.

$$K = FV^{-1} = \frac{1}{k_1 k_2 k_3 k_4} \begin{bmatrix} \lambda_2^0 S_h^0 \sigma k_3 k_4 & \lambda_2^0 S_h^0 k_1 k_3 k_4 & \lambda_1^0 S_h^0 \sigma_v k_1 k_3 k_4 & \lambda_1^0 S_h^0 k_1 k_2 k_3 \\ 0 & 0 & 0 & 0 \\ \lambda_v^0 S_v^0 \sigma k_3 k_4 & \lambda_v^0 S_v^0 k_1 k_3 k_4 & 0 & 0 \\ 0 & 0 & 0 & 0 \end{bmatrix} \quad (3)$$

$$\mathcal{R}_0 = \rho(FV^{-1}) = \frac{1}{2k_1 k_2 k_3 k_4} \left(\lambda_2^0 S_h^0 \sigma k_3 k_4 + \sqrt{(\lambda_2^0 S_h^0 \sigma k_3 k_4)^2 + 4\lambda_1^0 S_h^0 \sigma \lambda_v^0 S_v^0 \sigma_v k_1 k_2 k_3 k_4} \right) \quad (4)$$

$$= \frac{1}{2k_1 k_2 k_3 k_4} \left(\mathcal{R}_{0s} + \sqrt{(\mathcal{R}_{0s})^2 + 4\mathcal{R}_{0v}} \right) \quad (5)$$

In line 5, it can be clearly seen that the basic reproductive number for the entire system is composed of terms relating specifically to contributions from the vector and sexual transmission routes. Furthermore, threshold conditions for $\mathcal{R}_0 < 1$ are achieved when $\mathcal{R}_{0s} + \mathcal{R}_{0v} < 1$. As such, for the purposes of this paper, let $\mathcal{R}'_0 = \mathcal{R}_{0s} + \mathcal{R}_{0v}$ represent the basic reproductive number for the system.

As a direct consequence of using the next generation method, this disease-free equilibrium is locally asymptotically stable when $\mathcal{R}'_0 < 1$ and is unstable when $\mathcal{R}'_0 > 1$.

Elasticity Analysis

In this section, the impact of each parameter on the basic reproductive number is discussed. In order to compute the normalized sensitivity, or elasticity, for each parameter, p , the following formula was used.

$$E_p = \frac{\partial \mathcal{R}'_0}{\partial p} \times \frac{p}{\mathcal{R}'_0} \quad (6)$$

The elasticity for each parameter is given in [Table 2](#). To provide context for these numbers, positive values of elasticity indicate a direct relationship between the parameter and \mathcal{R}'_0 , while negative values indicate an inverse relationship. For example, an elasticity of +0.5 indicates that a 10% increase (decrease) in the value of that parameter will result in a 5% increase (decrease) in the value of \mathcal{R}'_0 . On the contrary, an elasticity of -0.5 indicates that a 10% increase (decrease) in the value of that parameter will result in a 5% decrease (increase) in \mathcal{R}'_0 .

Of these elasticities, the most notable is that of k_v . Thus far, in the comparison between the original model and the one being studied, analysis has yielded similar results. In the original model, however, the parameter associated with precautionary measures had an elasticity of -0.02234 (Biswas, 2019). In the proposed model, an elasticity of 0.49976 is observed for the parameter k_v . Recall that $k_v = (1 - \epsilon_v)$, so that higher rates of effectiveness serve to decrease k_v , hence the observation of a direct relationship between the two. In accounting separately for protective measures against Zika Virus, it appears that these measures are much more influential to the disease's basic reproductive number than initially indicated in the original model.

Table 2. Parameter elasticities for specified value					
Parameter	Value	Elasticity	Parameter	Value	Elasticity
b	0.45	0.999517	ε_s	0.004	NA
c	0.00071429	-0.0421137	ε_v	0.004	NA
k_s	0.996	0.00048295	μ	0.00019204	1.49795
k_v	0.996	0.499759	μ_v	0.02053120	-1.2105
r	0.00552894	0.00048295	π	0.00019204	-0.499759
α_1	0.04441746	0.499759	π_v	100	0.499759
α_2	0.03362689	0.00048295	σ	0.35808521	0.00026813
α_3	0.04791129	0.499759	σ_v	0.02070591	0.253093
γ	0.07098011	-0.498892			

Results

As stated previously, analysis of the proposed model has yielded results similar to that of the original; an outcome that was desired at the beginning of this project. In addition to the steady state analysis of the models, similar results were sought when running simulations with them. This section focuses on the results of running simulations with both models under near-identical conditions.

In these simulations, the parameter values used by Biswas (2019) were fed to the proposed model; a full list of the parameter values used can be found in [Table 2](#). For the newly introduced parameters, ε_s and ε_v , it was discovered that values less than 1% yielded the best comparison results, given that an awareness rate of 0.00000440 was used in the original model. Figure 2 displays the results of the comparison graphically.

In [Figure 3](#), nearly-identical behavior between the models can be observed in almost every class, except for susceptible and recovered hosts. In the graphs, however, it can be seen that the proposed model produced higher values for susceptible hosts and lower values for recovered hosts than the original model. This difference can be explained by the fact that, in the proposed model, susceptible hosts are not

constantly being transferred to the recovered class, a process which artificially lowers the number of susceptible individuals and inflates the number of recovered.

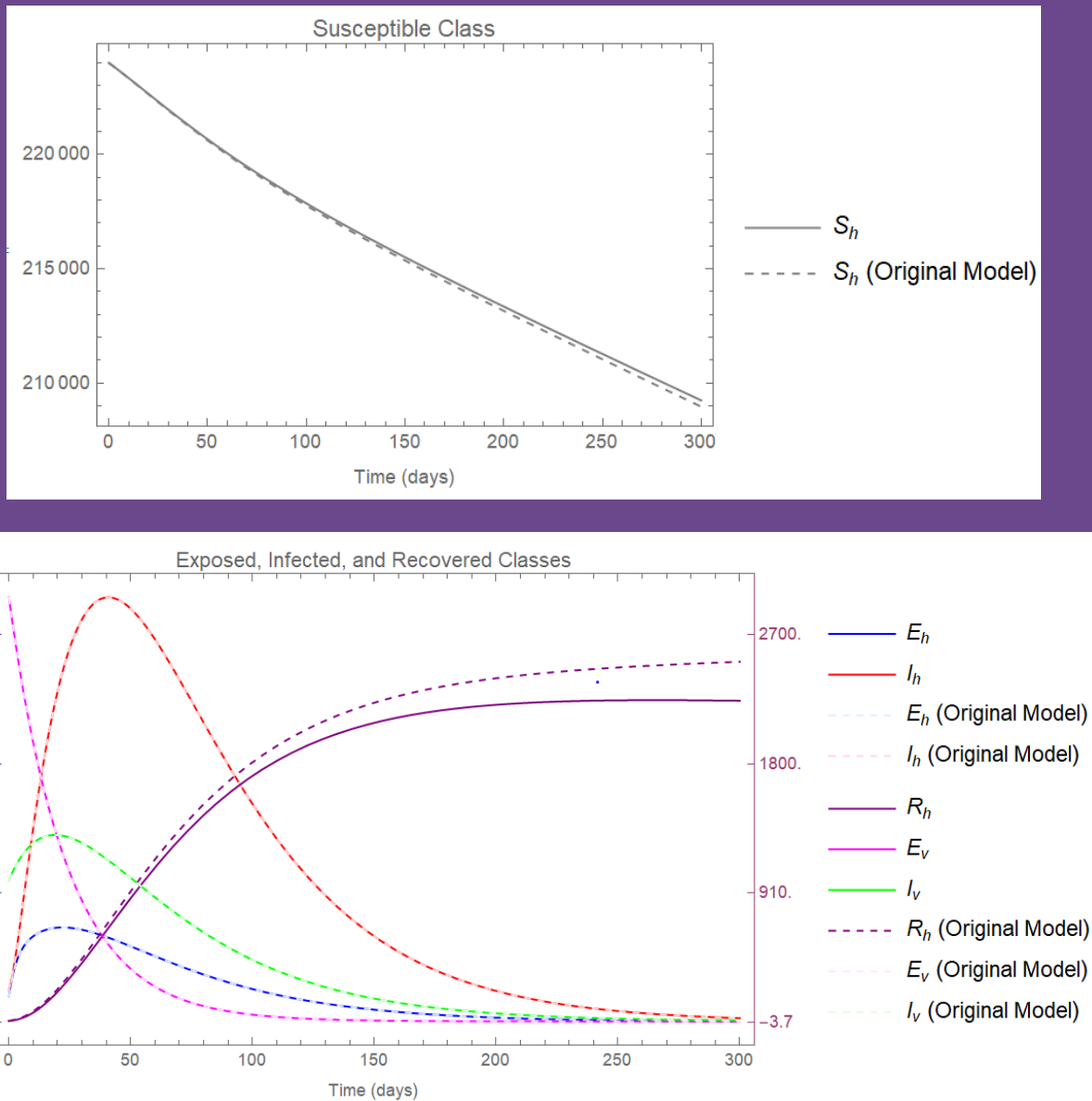


Figure 3. Simulation with both models under near-identical conditions

In order to draw attention to the fit of the proposed model to the original, a dual-axis coordinate system was used to capture the behavior of the exposed, infected, and recovered classes in a single plot. Additionally, population sizes for the exposed, infected, and recovered classes were scaled down considerably in order to make the graphs more readable.

Conclusion

In this paper, an existing Zika Virus model was modified in an effort to make it both more intuitive and more accurate. Disease free analysis of the proposed system showed that, as in the original model, the DFE is locally asymptotically stable for $\mathcal{R}_0 < 1$. Additionally, it has been shown that the proposed model behaves almost identically to the original under similar conditions and initial values. Based on these results, it appears that the modifications made were able to accomplish their goal without having a significant impact on the behavior of the system; simulations indicate that the only divergence experienced between the models occurs in the susceptible and recovered host populations, but this divergence is expected given the changes made.

Sensitivity analysis of the proposed system showed that one of the newly introduced parameters, k_v , had a much larger impact on the value of the basic reproductive number than the parameter associated with disease prevention in the original model. Additionally, by considering disease prevention methods separately for each mode of transmission, these measures can be more accurately accounted for in the model. Given the difference in sensitivities between the parameters k_s and k_v , correctly identifying the effectiveness of the preventative measures appears to be of great value.

Further work on this project would include additional analysis of the model. Thus far, only local asymptotic stability of the DFE has been shown. Given the similarities seen between the models throughout this project, it is expected that further steady state analysis of the proposed system would yield similar results to that of Biswas et al. (2019). This includes proving global asymptotic stability of the DFE, as well the

existence and stability of an endemic equilibrium. Finally, the original model experienced backwards bifurcation, indicating that $\mathcal{R}_0 < 1$ is a necessary condition for the stability of the DFE, but is not alone sufficient. At this time, whether the proposed exhibits this property is unknown.

References

- [1] Augusto FB, Bewick S, Fagan WF. Mathematical model of Zika virus with vertical transmission. *Infect Dis Model*. 2017 May 23;2(2):244-267. doi: 10.1016/j.idm.2017.05.003. PMID: 29928740; PMCID: PMC6001972.
- [2] Biswas, S. K., Ghosh, U., & Sarkar, S. (2019). Mathematical model of zika virus dynamics with vector control and sensitivity analysis. *Infectious Disease Modelling*, 5, 23–41. <https://doi.org/10.1016/j.idm.2019.12.001>.
- [3] Bonyah, E., & Okosun, K. O. (2016). Mathematical modeling of Zika virus. *Asian Pacific Journal of Tropical Disease*, 6(9), 673–679. [https://doi.org/10.1016/s2222-1808\(16\)61108-8](https://doi.org/10.1016/s2222-1808(16)61108-8).
- [4] Casale TB, Teng MN, Morano JP, Unnasch T, Lockwood CJ. Zika virus: An emerging infectious disease with serious perinatal and neurologic complications. *J Allergy Clin Immunol*. 2018 Feb;141(2):482-490. doi: 10.1016/j.jaci.2017.11.029. Epub 2017 Dec 19. PMID: 29273403.
- [5] Centers for Disease Control and Prevention. (2019, May 14). *Birth Defects*. Centers for Disease Control and Prevention. https://www.cdc.gov/zika/healtheffects/birth_defects.html.
- [6] Centers for Disease Control and Prevention. (2019, May 14). *Zika and Guillain-Barré Syndrome*. Centers for Disease Control and Prevention. <https://www.cdc.gov/zika/healtheffects/gbs-qa.html>.
- [7] Centers for Disease Control and Prevention. (2019, May 21). *Symptoms*. Centers for Disease Control and Prevention. <https://www.cdc.gov/zika/symptoms/symptoms.html>.
- [8] Lowe, R., Barcellos, C., Brasil, P., Cruz, O., Honório, N., Kuper, H., & Carvalho, M. (2018). The Zika Virus Epidemic in Brazil: From Discovery to Future Implications. *International Journal of Environmental Research and Public Health*, 15(1), 96. <https://doi.org/10.3390/ijerph15010096>.
- [9] Peiter PC, Pereira RdS, Nunes Moreira MC, Nascimento M, Tavares MdFL, Franco VdC, et al. (2020) Zika epidemic and microcephaly in Brazil: Challenges for access to health care and promotion in three epidemic areas. *PLoS ONE* 15(7): e0235010. <https://doi.org/10.1371/journal.pone.0235010>.
- [10] Rahman, M., Bekele-Maxwell, K., Cates, L.L. *et al*. Modeling Zika Virus Transmission Dynamics: Parameter Estimates, Disease Characteristics, and Prevention. *Sci Rep* 9, 10575 (2019). <https://doi.org/10.1038/s41598-019-46218-4>.
- [11] Ryan SJ, Carlson CJ, Mordecai EA, Johnson LR (2019) Global expansion and redistribution of *Aedes*-borne virus transmission risk with climate change. *PLoS Negl Trop Dis* 13(3): e0007213. <https://doi.org/10.1371/journal.pntd.0007213>.
- [12] Suparit, P., Wiratsudakul, A., & Modchang, C. (2018). A mathematical model for Zika virus transmission dynamics with a time-dependent mosquito biting rate. *Theoretical biology & medical modelling*, 15(1), 11. <https://doi.org/10.1186/s12976-018-0083-z>.